Human Molecular Genetics, 2008, Vol. 17, No. 24 ***4001–4011***
doi:10.1093/hmg/ddn303
Advance Access published on September 19, 2008

Mitochondrial DNA background modulates the assembly kinetics of OXPHOS complexes in a cellular model of mitochondrial disease

Rosa Pello[1,2], Miguel A. Martín[1,2], Valerio Carelli[3], Leo G. Nijtmans[4], Alessandro Achilli[5,6], Maria Pala[5], Antonio Torroni[5], Aurora Gómez-Durán[7,8], Eduardo Ruiz-Pesini[7,8], Andrea Martinuzzi[9], Jan A. Smeitink[4], Joaquín Arenas[1,2] and Cristina Ugalde[1,2,*]

[1]CIBERER-U723 and [2]Centro de Investigación, Hospital Universitario 12 de Octubre, Madrid 28041, Spain, [3]Dipartimento di Scienze Neurologiche, Università di Bologna, Bologna 40123, Italy, [4]Nijmegen Centre for Mitochondrial Disorders, Radboud University Nijmegen Medical Centre, Nijmegen 6500 HB, The Netherlands, [5]Dipartimento di Genetica e Microbiologia, Università di Pavia, Pavia 27100, Italy, [6]Dipartimento di Biologia Cellulare e Ambientale, Università di Perugia, Perugia 06123, Italy, [7]CIBERER-U727 and [8]Departamento de Bioquímica, Biología Molecular y Celular, Universidad de Zaragoza, Zaragoza 50013, Spain and [9]E. Medea Scientific Institute, Conegliano Research Centre, Conegliano 21015, Italy

Received August 7, 2008; Revised and Accepted September 16, 2008

Leber's hereditary optic neuropathy (LHON), the most frequent mitochondrial disorder, is mostly due to three mitochondrial DNA (mtDNA) mutations in respiratory chain complex I subunit genes: 3460/*ND1*, 11778/*ND4* and 14484/*ND6*. Despite considerable clinical evidences, a genetic modifying role of the mtDNA haplogroup background in the clinical expression of LHON remains experimentally unproven. We investigated the effect of mtDNA haplogroups on the assembly of oxidative phosphorylation (OXPHOS) complexes in transmitochondrial hybrids (cybrids) harboring the three common LHON mutations. The steady-state levels of respiratory chain complexes appeared normal in mutant cybrids. However, an accumulation of low molecular weight subcomplexes suggested a complex I assembly/stability defect, which was further demonstrated by reversibly inhibiting mitochondrial protein translation with doxycycline. Our results showed differentially delayed assembly rates of respiratory chain complexes I, III and IV amongst mutants belonging to different mtDNA haplogroups, revealing that specific mtDNA polymorphisms may modify the pathogenic potential of LHON mutations by affecting the overall assembly kinetics of OXPHOS complexes.

INTRODUCTION

Leber's hereditary optic neuropathy (LHON, MIM#535000) is a maternally inherited blinding disease characterized by subacute degeneration of retinal ganglion cells (RGCs) leading to optic nerve atrophy and bilateral loss of central vision, prevalently in young males (1). In ~95% of cases worldwide, LHON is caused by three point mutations in mitochondrial DNA (mtDNA) respiratory chain complex I subunit genes: m.3460G > A in *ND1* (3460/*ND1*), m.11778G > A in *ND4* (11778/*ND4*), and m.14484T > C in *ND6* (14484/*ND6*) (2). Although the genetic basis are known since 1988 (3), the pathogenesis of LHON via complex I dysfunction remains poorly understood. Most LHON families carry the mtDNA pathogenic mutation in homoplasmic condition, but not all maternally related individuals develop visual loss, suggesting additional genetic or epigenetic determinants for the phenotypic

*To whom correspondence should be addressed at: Centro de Investigación, Hospital Universitario 12 de Octubre, Avda. de Córdoba s/n, Madrid 28041, Spain. Tel: +34 913908763; Fax: +34 913908544; Email: cugalde@h12o.es
New Genbank accession numbers: EU915472, EU915473, EU915474, EU915475, EU915476, EU915477, EU915478, EU915479, FJ178379, FJ178380

expression of LHON. To date, the most compelling evidence for a genetic modifying role comes from the mtDNA haplogroup hosting the primary LHON mutations. Independent studies revealed that the Eurasian haplogroup J is preferentially associated with the 11778/*ND4* and 14484/*ND6* LHON pathogenic mutations (4–6). Recently, this association was narrowed to haplogroup J1 for the 14484 mutation, and to subclades J1c and J2b for the 11778 mutation, suggesting that specific mutational motifs, which included non-synonymous variants in complex I and III subunit genes, could increase the penetrance and risk of LHON expression by structural alterations in the mitochondrial respiratory chain complexes or supercomplexes (7,8).

Due to the lack of animal models to study mitochondrial disorders caused by mtDNA gene defects, transmitochondrial cytoplasmic hybrids (cybrids) have become a major cellular model to analyze the pathophysiological consequences of LHON mutations. Cybrids are generated by fusing mtDNA-depleted human cells (rho zero cells) with enucleated cells (cytoplasts) from LHON patients. The resulting cybrid clones contain a uniform nuclear DNA (nDNA) and an exogenous mtDNA harboring the LHON mutation of interest, allowing direct comparisons of biochemical phenotypes due solely to different mtDNA species (9). Bioenergetics studies demonstrated that the 3460/*ND1* mutation, associated with the most severe clinical phenotype (10), consistently led to a complex I activity decrease, while the 11778/*ND4* and 14484/*ND6* mutations presented normal or slightly reduced activities in both patients and cybrids (11–14). Complex I-dependent (pyruvate or glutamate-malate) respiration studies showed a variable reduction in the oxygen consumption rates depending on the mutation (11,12,14,15), which was accompanied by a severe impairment of complex I-driven ATP synthesis (15). A prevalent role of increased reactive oxygen species (ROS) production in LHON pathogenesis was proposed (16,17), as well as a decrease in antioxidant defenses that was particularly evident for the 3460/*ND1* and 11778/*ND4* mutations (18). Moreover, incubation of LHON cybrids in galactose medium impaired cell growth and caused massive apoptotic cell death, being the 3460/*ND1* and 14484/*ND6* mutations more susceptible to apoptosis than the 11778/*ND4* mutation (12,18,19).

In the present study, we have investigated control and LHON cybrids in which the mtDNA genome was completely sequenced. By using blue native gel electrophoresis (BN–PAGE) in combination with immunodetection, we aimed to elucidate the effect that common primary LHON mutations on different mtDNA haplogroups might exert on the assembly of complex I and other mitochondrial respiratory chain complexes. To address the dynamics of assembly, we partially depleted control and LHON cybrids of oxidative phosphorylation (OXPHOS) complexes by doxycycline treatment, which reversibly inhibits mitochondrial translation. Our results showed altered kinetics of complex I assembly and defective recovery of complex I activity in all LHON cybrids, and differential alterations in the assembly kinetics of respiratory chain complexes III and IV that can be attributed to specific genetic variations amongst the mtDNA backgrounds hosting the primary LHON mutations.

RESULTS

Cybrid clones and complete sequence analysis of mtDNA

In the present study we have used six homoplasmic mutant LHON cybrid cell lines (two for each common mutation), previously investigated and extensively characterized (11,15,17–19) and four control cybrid cell lines. In all cases the complete sequence of the cybrid-repopulating mtDNAs was determined. All non-synonymous polymorphic variants found in the mtDNA coding regions relative to the revised Cambridge reference sequence (20) are listed in Table 1.

Steady-state levels of individual respiratory chain complexes in LHON cybrids

To analyze the respiratory chain content in the four control and six mutant cybrids harboring different mtDNA backgrounds (Table 1), we performed BN–PAGE combined with complex I *in-gel* activity (IGA) assay and western blot analysis with antibodies raised against specific OXPHOS subunits (Fig. 1A). Normal complex I activities were found in all cybrids, and no significant differences were observed in the steady-state levels of fully assembled complexes I, III and IV between controls and mutants. For complex II, a relative lower signal was found in the 11778/*ND4* mutant clones (Fig. 1A, lowest panel), which might reflect a decreased amount of mitochondria as suggested by the previously reported decreased citrate synthase activity of these clones compared with controls (15). The rest of cybrid clones showed comparable complex II expression levels, which correlated with their normal citrate synthase activities (15). In order to exclude expression differences among the clones due to variations in their mitochondrial mass, the signal obtained from the complex II antibody was used to normalize for the expression levels of mitochondrial respiratory chain complexes (Fig. 1B). No significant differences were observed among control cybrids belonging to different haplogroups. A general tendency for higher complex I activity or expression levels of mitochondrial complexes I, III and IV, and for the supercomplex $CIII_2$+ CIV (but not complex II) was observed in the haplogroup J1 mutant cells. This increase was not statistically significant for the clones characterized by the 14484/*ND6* mutation on haplogroup J1 (ND6/J1 and ND6/J1′). However, the clone carrying the 11778/*ND4* mutation on haplogroup J1 (ND4/J1) showed significantly higher steady-state levels ($P < 0.05$) of all respiratory chain complexes when compared with the controls or to its counterpart ND4/U5, which harbored the same mutation on a haplogroup U5a mtDNA. Clone ND4/U5 on the contrary did not show significant differences when compared with controls. Similarly, no significant differences were found in the expression levels of respiratory chain complexes I, III, and IV between controls and the clones harboring the 3460/*ND1* mutation on different subclades (H* and H12) of haplogroup H. A ~4-fold decrease ($P < 0.05$) in the expression levels of supercomplex $CIII_2$+ CIV was observed in clone ND1/H12, but this result did not correlate with a decreased expression of individual complexes III or IV (Fig. 1B).

The mtDNA copy number was calculated for each clone in order to exclude that the differences in the steady-state

Table 1. Haplogroup affiliation and non-synonymous nucleotide changes of mtDNAs from the cybrid clones used in this study

Cybrid cell lines	Genbank ID	LHON mutation	Haplogroup	Non-synonymous polymorphisms relative to rCRS[a]	Amino acid change
CON/T2	FJ178379	Control	T2	T4216C (*ND1*)	Tyr>Hi
				A4917G (*ND2*)	Asn>Asp
				A10398G (*ND3*)[b]	Thr>Ala
				C14766T (*CYTB*)	Thr>Ile
				C15452A (*CYTB*)	Leu>Ile
CON/J1[c]	FJ178380	Control	J1b	T4216C (*ND1*)	Tyr>His
				A4917G (*ND2*)[c]	Asn>Asp
				G5460A (*ND2*)	Ala>Thr
				G8557A (*ATP6*)	Ala>Thr
				A10398G (*ND3*)	Thr>Ala
				G13708A (*ND5*)	Ala>Thr
				T13879C (*ND5*)	Ser>Pro
				C14766T (*CYTB*)	Thr>Ile
				C15452A (*CYTB*)	Leu>Ile
CON/K1	EU915473	Control	K1a2	A4024T (*ND1*)	Thr>Ser
				G9055A (*ATP6*)	Ala>Thr
				A10398G (*ND3*)	Thr>Ala
				T11025C (*ND4*)	Leu>Pro
				C14766T (*CYTB*)	Thr>Ile
				T14798C (*CYTB*)	Phe>Leu
CON/H5	EU915472	Control	H5	A7245G (*COI*)	Thr>Ala
ND1/H*	EU915474	G3460A	H*	–	–
ND1/H12	EU915475	G3460A	H12	A14552G (*ND6*)	Val>Ala
ND4/J1	EU915476	G11778A	J1c	T4216C (*ND1*)	Tyr > His
				A10398G (*ND3*)	Thr > Ala
				T12083G (*ND4*)	Ser > Ala
				G13708A (*ND5*)	Ala > Thr
				C14766T (*CYTB*)	Thr > Ile
				T14798C (*CYTB*)	Phe > Leu
				C15452A (*CYTB*)	Leu > Ile
ND4/U5	EU915477	G11778A	U5a	G9477A (*COIII*)	Val > Ile
				A9667G (*COIII*)	Asn > Ser
				C14766T (*CYTB*)	Thr > Ile
				A14793G (*CYTB*)	His > Arg
ND6/J1	EU915478	T14484C	J1b	T4216C (*ND1*)	Tyr > His
				G5460A (*ND2*)	Ala > Thr
				G8557A (*ATP6*)	Ala > Thr
				A10398G (*ND3*)	Thr > Ala
				G13708A (*ND5*)	Ala > Thr
				T13879C (*ND5*)	Ser > Pro
				C14766T (*CYTB*)	Thr > Ile
				C15452A (*CYTB*)	Leu > Ile
ND6/J1′	EU915479	T14484C	J1c	T4216C (*ND1*)	Tyr > His
				T7042C (*COI*)	Val > Ala
				A10398G (*ND3*)	Thr > Ala
				G13708A (*ND5*)	Ala > Thr
				G14279A (*ND6*)	Ser > Leu
				C14766T (*CYTB*)	Thr > Ile
				T14798C (*CYTB*)	Phe > Leu
				C15452A (*CYTB*)	Leu > Ile

[a]rCRS refers to the revised Cambridge reference sequence (20). In addition, all mtDNAs differed from rCRS, which belongs to haplogroup H2a, for A8860G (*ATP6*) and A15326G (*CYTB*).
[b]The 10398 polymorphism in CON/T2, and
[c]the 4917 polymorphism in CON/J1, have been confirmed by RFLP analysis and sequencing. Both 10398 and 10463 ($tRNA^{Arg}$) polymorphisms, and both 4917 and 5460 polymorphisms, were present in the same electropherogram without double peaks.

expression levels of respiratory chain complexes were influenced by variations in the mtDNA content among individual clones. No significant differences were found in the mtDNA/nDNA ratio between controls belonging to different haplogroups (Table 2). Although no differences were found between controls and clone ND1/H*, the rest of LHON mutant cybrids showed either increased or reduced mtDNA content. Clones ND1/H12, ND4/U5 and ND4/J1 exhibited the highest mtDNA/nDNA rates. These cells consistently showed the lowest relative levels of complex II or citrate synthase activities (15), suggesting that the high mtDNA content might represent a compensatory mechanism for the reduced mitochondrial mass. On the contrary, the 14484/*ND6* mutant clones exhibited the lowest mtDNA/nDNA rates but showed normal levels of complex II or citrate synthase activities. These relative differences in the mtDNA content did not seem to influence the steady-state levels of respiratory chain complexes in any clone except ND4/J1, which showed a significant increase in the expression levels of OXPHOS complexes. These expression differences might be due to the presence in each individual clone of specific polymorphisms in the D-loop control region or within the non-protein coding regions of mtDNA, such as the 12S and 16S rRNAs and the mitochondrial tRNAs. Polymorphic variations within these regions might affect the translation efficiency of mitochondrial proteins, which could account for the differences observed in the steady-state levels of the native OXPHOS complexes.

Differential accumulation of low molecular weight complex I subcomplexes in mutated LHON cybrids

In order to study whether the primary LHON mutations in the mitochondrial *ND1*, *ND4* and *ND6* genes could affect complex I assembly or stability, and to investigate the possible presence of complex I assembly intermediates or breakdown products, two-dimensional (2D) BN/SDS–PAGE electrophoresis was performed. Gels were blotted and incubated with an antibody against the complex I NDUFA9 subunit (Fig. 2). Each mutant cell line was compared with a control belonging to the closest evolutionarily related mtDNA haplogroup. Cybrids harboring the 3460/*ND1* mutation on haplogroup H12 mtDNA (ND1/H12) showed a smeary pattern of accumulated NDUFA9 subunit-containing subcomplexes, suggestive of a complex I assembly or stability defect, while the haplogroup H* clone (ND1/H*) showed normal amounts of fully assembled complex I and a regular pattern of low molecular weight subcomplexes. The same observation was made for the 11778/*ND4* mutation clones: the haplogroup U5a cybrid (ND4/U5a), showed an accumulation of NDUFA9-containing subcomplexes compared with its K1a control (K is a subclade of haplogroup U), while the haplogroup J1 clone (ND4/J1) showed normal amounts of fully assembled complex I and no accumulation of low molecular weight subcomplexes relative to the J1 control. A normal complex I assembly pattern was also observed for the 14484/*ND6* LHON mutation clones characterized by a J1 mtDNA. Our results suggest that the assembly and/or stability of mitochondrial respiratory chain complex I would be more severely affected by the primary LHON mutations when associated with certain mtDNA backgrounds, such as H12 or U5a, while the same mutation on a different haplogroup would cause a less severe disturbance on complex I.

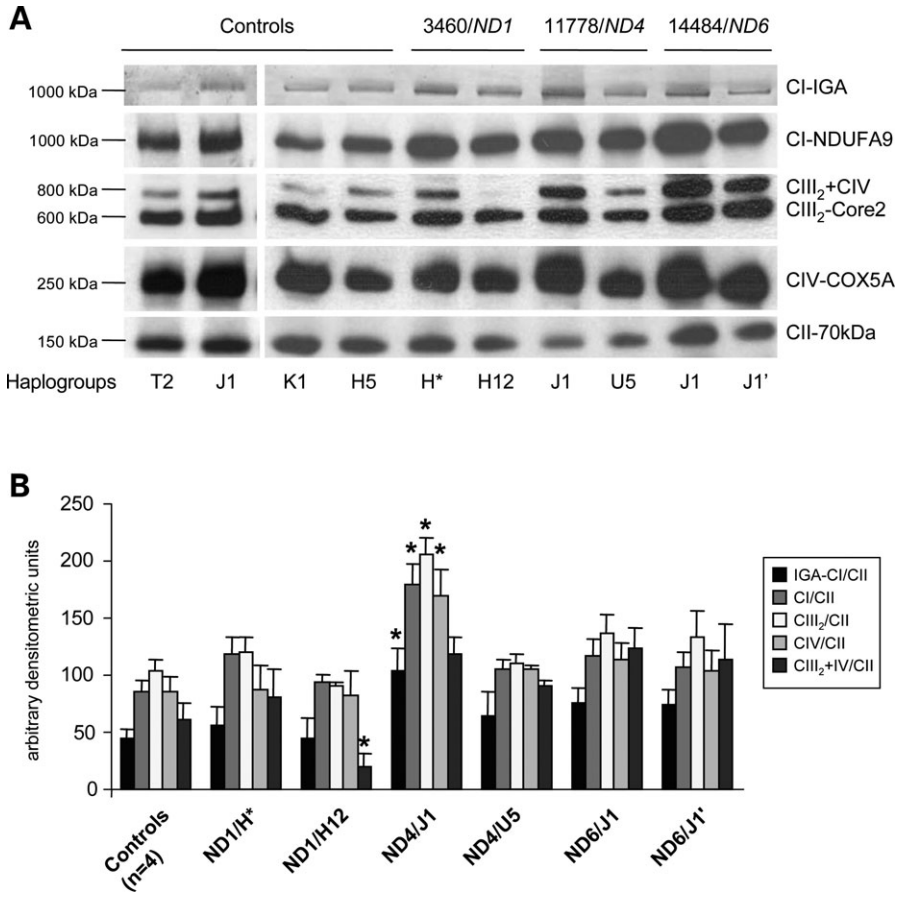

Figure 1. (**A**) BN–PAGE analysis of mitochondrial respiratory chain complexes in control and LHON cybrids. Mitochondrial particles were isolated as described in Materials and Methods and 40 μg protein was analyzed on a 5–15% BN–PAGE for the separation of multisubunit complexes. First panel, complex I IGA assay. A second gel was run in duplicate and western blot analysis was performed using antibodies against complex I NDUFA9 subunit (second panel), complex III core2 protein (third panel), complex IV COX5A subunit (fourth panel), or complex II-70 kDa subunit (fifth panel). CI, fully assembled complex I; $CIII_2$, complex III dimer; CIV, complex IV; $CIII_2 + CIV$ indicates the presence of a supercomplex containing complexes III and IV, frequently observed on BN–PAGE. (**B**) To calculate the steady-state levels of complex I activity and fully assembled complexes I, III, IV and supercomplex $CIII_2 + CIV$, five independent blue native blots were quantified, and the average numerical values normalized to those obtained from complex II. Significant differences (*t*-student, $P < 0.05$) are highlighted with an asterisk.

Table 2. MtDNA copy number in cybrid cell lines expressed as mtDNA/nDNA ratio

Cybrid cell lines	mtDNA/nDNA
143B TK$^-$206	381 ± 20
Controls ($n = 4$)	355 ± 44
ND1/H*	395 ± 36
ND1/H12	517 ± 62
ND4/J1	639 ± 35
ND4/U5	553 ± 32
ND6/J1	243 ± 26
ND6/J1′	239 ± 20
143B rho zero	n.d.

Numbers indicate the mean values of four independent measurements per sample ± standard deviation; n.d., not-detectable.

Assembly kinetics of respiratory chain complexes in control cybrids

In order to analyze possible differences in the assembly kinetics of respiratory chain complexes in control cybrids with different mtDNA backgrounds, we depleted the cells of complex I and other OXPHOS complexes containing mitochondrial-encoded subunits, by reversibly blocking mitochondrial protein translation with doxycycline. This strategy was successfully used to follow the assembly kinetics of respiratory chain complex I in the parental 143B TK$^-$206 cell line (21), and helped the interpretation of assembly defects in complex I-deficient patients with mutations in structural genes (22). Because further treatment with doxycycline affected cell viability in our culture conditions, cells were cultured for 6 days in the presence of the inhibitor. After the release of drug inhibition, cells grown in exponential conditions started translating mitochondrial proteins, and the assembly of newly synthesized respiratory chain complexes was investigated. To follow the reappearance of mitochondrial complexes after the reversible block of assembly, samples were collected at different time points (0, 6, 15, 24, 48, 72 and 96 h) after doxycycline removal, run on BN–PAGE and assayed for complex I IGA, or alternatively, blotted on nitrocellulose and incubated with antibodies raised against specific OXPHOS subunits. Results showed no significant differences

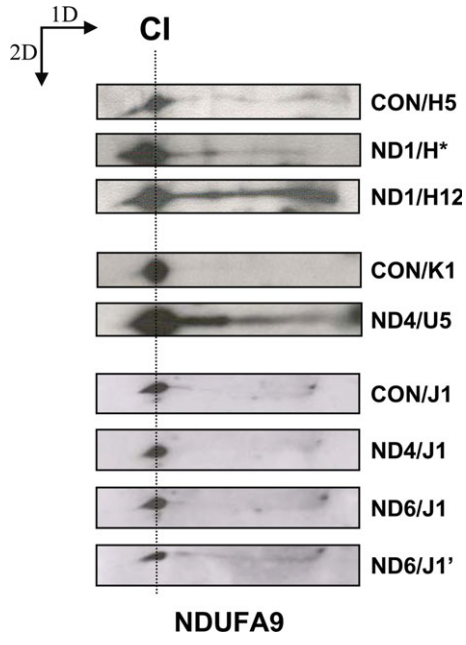

Figure 2. 2D-BN/SDS–PAGE analysis of mitochondrial respiratory complex I in LHON mutants. For the separation of individual subunits a 10% tricine SDS-gel was run in the second dimension. Gels were blotted. For the positioning of complex I (~980 kDa) a primary antibody against complex I subunit NDUFA9 (39 kDa) was used in control and mutant cybrids. CI indicates the relative position of fully assembled complex I. The directions of the first (1D) and second (2D) dimension are shown.

in the recovery kinetics of respiratory chain complexes among control cybrids belonging to different haplogroups (data not shown). For this reason, we quantified the signals obtained from the IGA assays and western blots in the four independent control cell lines, normalized them for the expression levels of mitochondrial complex II, expressed them as a percentage of the untreated cells (which correspond to the steady-state expression levels), and calculated the average numerical values for the complex I activity restoration curve and the assembly rates of respiratory chain complexes I, III, IV and supercomplex $CIII_2$+ CIV (Fig. 3).

Consistent with previous observations, after 6 days of doxycycline treatment (Fig. 3, T0 point), we observed ~70–90% reduction of complex I activity or fully assembled respiratory chain complexes in control cybrids compared with untreated cells (Fig. 3, SS point) (21). As shown in Figure 3A, controls mainly acquired fully assembled complex I between 24 and 48 h after doxycycline removal, and gained complex I activity 48 h after removing the drug. Restoration to normal complex I steady-state levels occurred at time 72–96 h, and normal complex I activity levels were reached at 96 h. The observed time course for complex I assembly and activity was comparable with previous findings (21,23,24). Fully assembled complex III was restored in a similar time course as complex I (Fig. 3B). Fully assembled complex IV, however, was acquired ~24 h later than complexes I and III (Fig. 3C). Similarly, the formation of the mitochondrial supercomplex $CIII_2$+ CIV paralleled the complex IV assembly kinetics, suggesting that a minimum pool of individual complexes III and IV is necessary in order to form supercomplex $CIII_2$+ CIV (Fig. 3C). Restoration to normal complex IV and supercomplex $CIII_2$+ CIV steady-state levels occurred 96 h after removing the drug. These results match other studies in which no bioenergetic differences were observed in control cybrid cell lines carrying European mtDNA haplogroups (25,26).

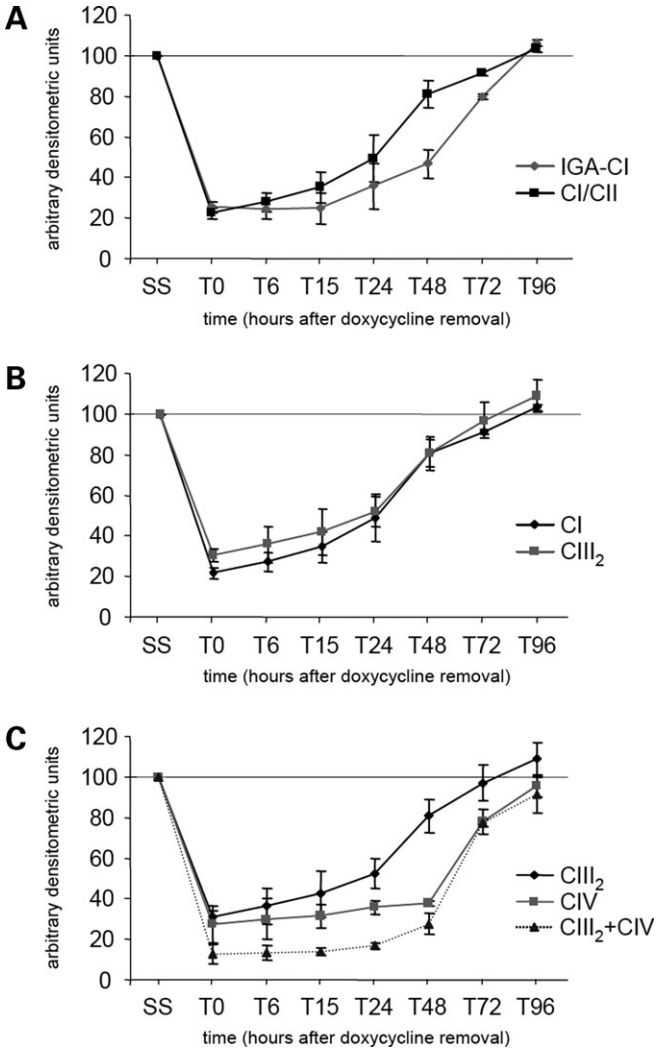

Figure 3. Assembly kinetics of respiratory chain complexes in control cybrids. The four controls used in this study were treated for 6 days with doxycycline (an inhibitor of mitochondrial translation), the medium was replaced by doxycycline-free medium and cells were grown for the indicated time (in hours). Forty microgram of crude mitochondrial pellets was analyzed by BN–PAGE in combination with complex I-IGA assay. Duplicate gels were blotted and incubated with antibodies against the NDUFA9 complex I subunit, complex III core2 protein, complex IV COX5A subunit and complex II-70 kDa subunit (data not shown). The signals were quantified, expressed as percentage of the untreated cells (indicated as SS), normalized with the complex II-70 kDa subunit and plotted. (**A**) Complex I activity recovery kinetics versus complex I assembly rates. (**B**) Complex I versus complex III assembly rates. (**C**) Complex III versus complex IV and supercomplex $CIII_2$ + CIV assembly kinetics.

Delayed assembly kinetics of respiratory chain complex I in cybrids harboring LHON primary mutations

To check whether the assembly kinetics of respiratory chain complex I was affected by the LHON mutations, we used

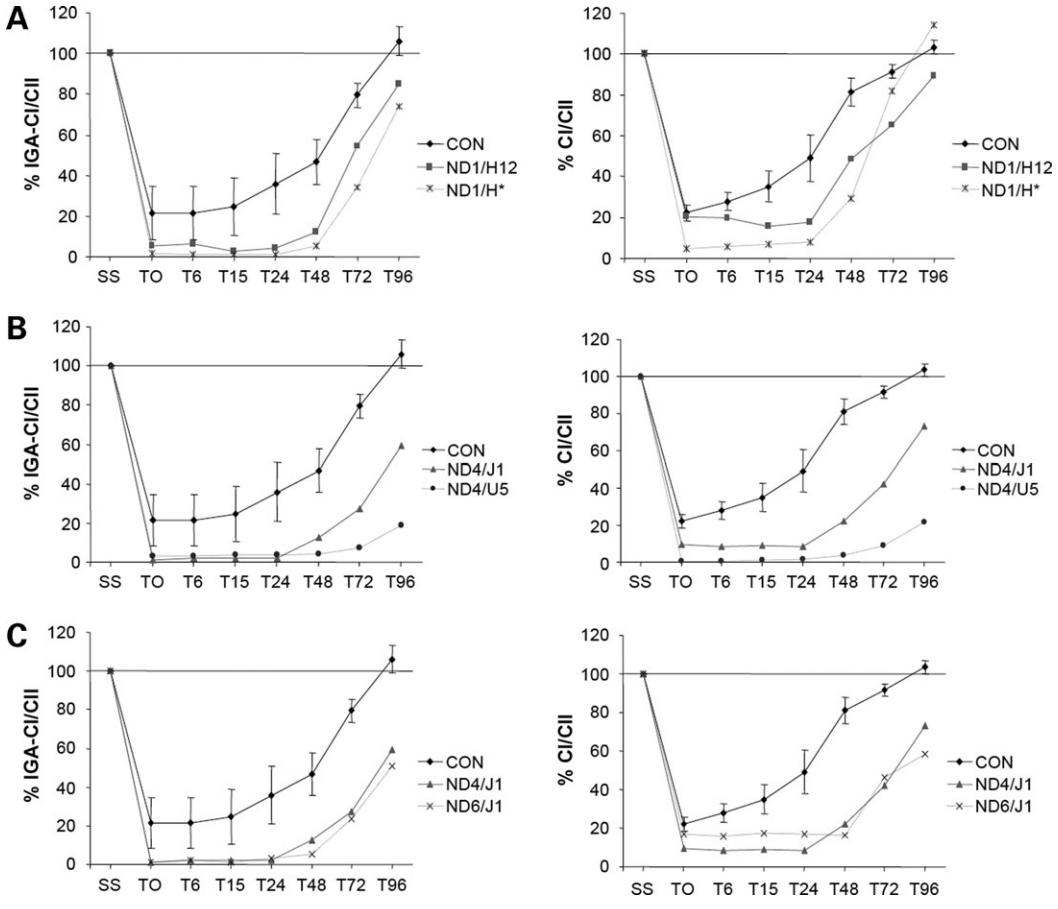

Figure 4. Re-appearance of respiratory chain complex I in LHON cybrids. The signals corresponding to complex I-IGA assays and western blots incubated with the NDUFA9 antibody (Supplementary Material, Figure S1) were quantified, expressed as percentage of the untreated cells (indicated as SS), normalized with the complex II-70 kDa subunit, plotted, and compared with the average assembly kinetics of the controls. (**A**) Clones ND1/H* and ND1/H12, harboring the 3460/*ND1* mutation on subclades H* and H12, respectively. (**B**) Clones ND4/J1 and ND4/U5, harboring the 11778/*ND4* mutation on haplogroups J1 and U5a, respectively. (**C**) Clones ND4/J1 and ND6/J1, harboring the 11778/*ND4* and 14484/*ND6* mutations on haplogroup J1 mtDNAs.

the same doxycycline inhibition strategy in our mutant cybrids (Supplementary Material, Figure S1). The complex I signals from blue native experiments were quantified, and normalized as previously mentioned. Cell lines were grouped according to the LHON mutation they harbored and compared with the 'average' control numerical values. After 6 days of doxycycline treatment (Fig. 4, T0 points), we observed a practically total reduction of complex I activity and ~85–100% reduction of fully assembled respiratory chain complex I in the mutant cybrids compared with the untreated cells (Fig. 4, SS points). These values contrast with those obtained for the controls during the inhibition process, suggesting that LHON mutations probably affect complex I stability.

Differences were found in the assembly kinetics of respiratory chain complex I between controls and LHON mutants. Clones characterized by the 3460/*ND1* mutation on haplogroups H12 and H* (ND1/H12 and ND1/H*, respectively) showed a similar 24 h delay in the recovery of complex I activity compared with controls (Fig. 4A, left). Controls gained ~50% of total complex I activity 48 h after doxycycline removal, and the 3460/*ND1* clones between 72 and 96 h. At time 96 h, controls showed 100% of complex I activity, while clones ND1/H12 and ND1/H* recovered 75–85% of total complex I activity. Similar results were obtained for the recovery of fully assembled complex I (Fig. 4A, right). Controls gained ~50% of total holocomplex I at time 24 h, and the 3460/*ND1* clones between 48 and 72 h. From time 48 h on complex I assembly kinetics seemed to speed up in the mutants, since at time 96 h clone ND1/H12 recovered ~90% of total holocomplex I, and the ND1/H* clone presented more fully assembled complex I than the controls. This effect might represent a compensatory mechanism as a response to the inhibition of mitochondrial protein synthesis. This might involve a general increase in mitochondrial mass because complex II, which only contains nuclear encoded subunits, also shows such an increase at 96 h in the ND1/H* cells (Supplementary Material, Figure S1).

Differences in the complex I assembly rates were detected between clones characterized by the 11778/*ND4* mutation on J1 and U5a haplogroups (Fig. 4B). Both the ND4/J1 and ND4/U5 cell lines showed a minimum of 48 h delay in the recovery of complex I activity and fully assembled complex I compared with controls. Clone ND4/J1 gained ~50% of total complex I activity and fully assembled complex I between 72 and 96 h after the drug removal, but clone ND4/U5a could not even reach these levels at 96 h.

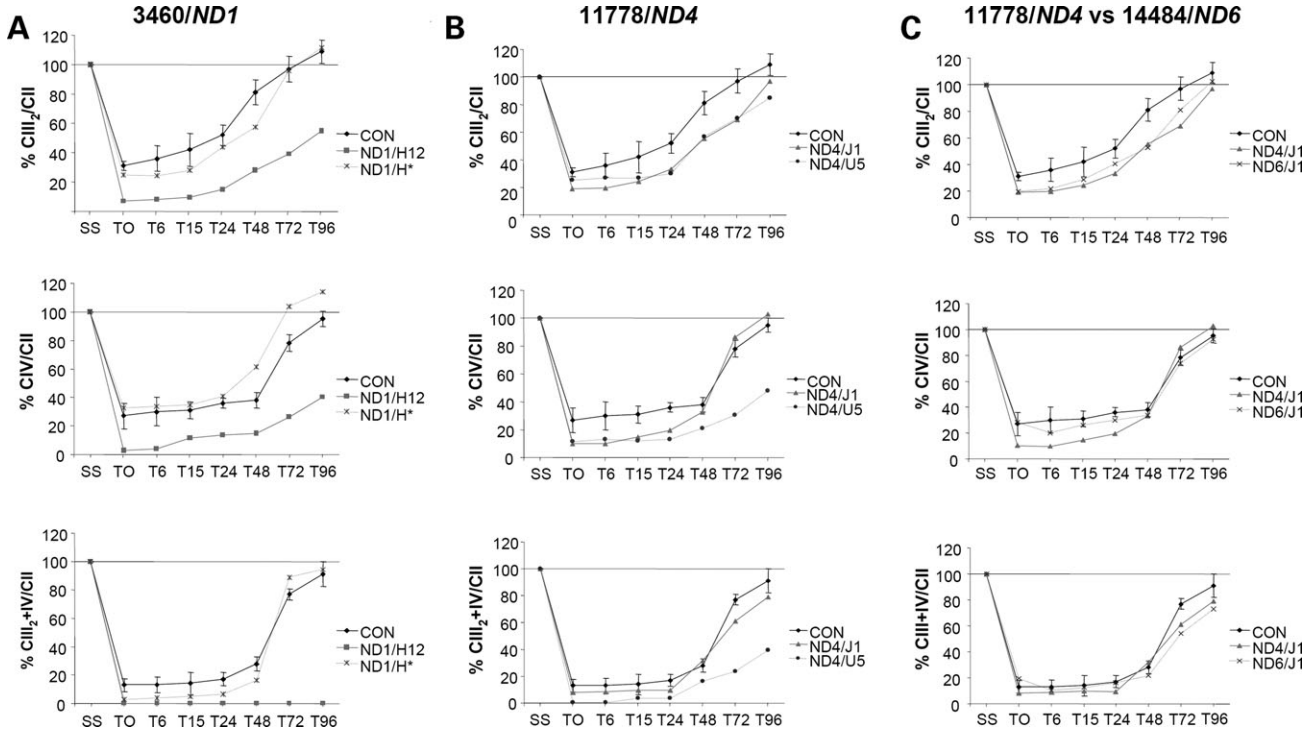

Figure 5. Assembly kinetics of respiratory chain complexes III and IV in LHON cybrids. The signals corresponding to western blots incubated with antibodies against the complex III core2 protein and complex IV COX5A subunit (Supplementary Material, Figure S1) were quantified, expressed as the percentage of untreated cells (indicated as SS), normalized with the complex II-70 kDa subunit, plotted, and compared with the control average assembly kinetics. (**A**) Signals corresponding to cybrid clones ND1/H* and ND1/H12, which harbor the 3460/*ND1* mutation. (**B**) Signals corresponding to cell lines ND4/J1 and ND4/U5 that harbor the 11778/*ND4* mutation. (**C**) Signals from cells harboring the 11778/*ND4* and 14484/*ND6* mutations on a haplogroup J1 mtDNA, which correspond to cell lines ND4/J1 and ND6/J1. Top graphs represent the complex III assembly curves. Middle graphs represent the complex IV assembly rates. Bottom graphs represent the supercomplex $CIII_2 + CIV$ assembly kinetics.

No differences were found in the complex I assembly kinetics of clones harboring the 14484/*ND6* mutation on a J1 mtDNA (data not shown). We next compared the 11778/*ND4* and 14484/*ND6* clones characterized by the same haplogroup J1 background (ND4/J1 and ND6/J1, respectively). Curiously, both clones showed similar delayed assembly kinetics of respiratory chain complex I (Fig. 4C). Our results demonstrate hampered kinetics of complex I assembly and activity recovery in all LHON cybrids.

MtDNA background influences the assembly kinetics of respiratory chain complexes III and IV in LHON cybrids

It has been suggested that the mitochondrial background, in particular subclades of haplogroups J or H that harbour specific polymorphisms in the *CYTB* gene, could interact synergistically with the primary LHON mutations, either altering the physical interaction between complexes I and III, or stabilizing the supercomplex $CI + CIII_2$ (7). Some alterations could add a negative effect on complex I function, since it has been reported that fully assembled complex III and lately, complex IV, are essential for the stability of mitochondrial complex I (27–29). For these reasons, we decided to test the assembly kinetics of respiratory chain complexes III and IV in our LHON cybrids (Fig. 5). Main differences were observed between the 3460/*ND1* mutant clones (Fig. 5A). Although no real differences were found in the recovery rates between clone ND1/H* and controls, the ND1/H12 cell line showed a minimum of 72 h delay in the recovery of fully assembled complex III (Fig. 5A, top). Controls gained ~50% of fully assembled complex III at time 24 h, whereas clone ND1/H12 reached these levels 96 h after doxycycline removal. Similarly, controls gained ~50% of total holocomplex IV between 24 and 48 h after doxycycline removal, whereas clone ND1/H12 could not reach these levels before 96 h (Fig. 5A, middle). In accordance with these results, clone ND1/H12 barely showed any expression of the mitochondrial supercomplex $CIII_2 + CIV$ (Fig. 5A, bottom).

Conversely both 11778/*ND4* clones only presented a slight delay in the complex III assembly kinetics relative to controls (Fig. 5B, top). At 96 h after doxycycline removal, clone ND4/J1 had recovered ~97% of total holocomplex III, and clone ND4/U5 ~85%. The main differences between these clones were found in the assembly kinetics of respiratory chain complex IV (Fig. 5B, middle). Mutant clone ND4/J1 presented no differences in the recovery kinetics of holocomplex IV, or supercomplex $CIII_2 + CIV$, with controls. However, the ND4/U5 cell line showed ~48 h delay in the recovery of fully assembled complex IV compared with ND4/J1 and controls. Controls gained ~50% of fully assembled complex IV between 48 and 72 h after doxycycline removal, whereas clone ND4/U5 almost reached these levels at 96 h. Similarly, the formation of the mitochondrial supercomplex $CIII_2 + CIV$ in the ND4/U5 clone paralleled the complex IV assembly time

course (Fig. 5B, bottom), with ~38% of the total amount of the supercomplex at time 96 h.

We next compared the ND4/J1 and ND6/J1 mutants (Fig. 5C). No differences were found in the assembly kinetics of any respiratory chain complex.

DISCUSSION

The cybrids used in this study have been extensively analyzed as a model to investigate LHON pathophysiology, providing substantial evidence of complex I-dependent defects in respiration, ATP synthesis, and increased ROS production (11,15,17–19). In the present investigation we have further analyzed the effect of the most common LHON mutations on the assembly or stability of native mitochondrial respiratory chain complexes, and checked whether different mitochondrial genetic backgrounds could affect this process.

Our results are two-fold. First, we show that steady-state levels of fully assembled complex I and other respiratory chain complexes are not decreased in LHON mutant cybrids, but complex I assembly kinetics is delayed and complex I stability is reduced by the LHON mutations. This is illustrated by differences in the complex I assembly profile in 2D-BN/SDS gels, increased complex I turnover in the LHON mutant cells after a 6 days incubation with doxycycline, and differences in the recovery kinetics of respiratory chain complex I among LHON clones. Secondly, this defect in complex I assembly/stability is further modified by the mtDNA haplogroup, and may be mediated by the assembly rates and stability of respiratory chain complexes III and IV. Thus, the present results provide the first experimental evidence that certain mtDNA haplogroups, in combination with the LHON pathogenic mutations, may contribute to the severity of this disease by shifting the assembly kinetics of respiratory chain complexes.

Our study also describes a useful mechanism to unveil assembly defects in patients with apparently normal respiratory chain enzyme activities. At first glance, the normal steady-state levels of fully assembled complex I in LHON mutant cybrids looked as if there is no effect of LHON primary mutations on the formation of this complex. However, a differential accumulation of complex I subassemblies in several mutants was suggestive of a complex I assembly or stability defect. This defect was more evident in cybrids harboring the 3460/*ND1* and 11778/*ND4* mutations on H12 and U5a haplogroups, while clones harboring the same mutations on a different mtDNA background showed normal amounts of fully assembled complex I, and a normal pattern of low molecular weight subcomplexes. These results suggest that, in LHON cybrids, the severity of the complex I assembly and/or stability defect might depend on the association of the primary LHON mutations with specific mtDNA backgrounds.

The analysis of respiratory chain complexes after a transient depletion of OXPHOS complexes with doxycycline further supported a decreased assembly or stability of complex I in the LHON mutants. Remarkably, after 6 days in the presence of the inhibitor all mutant cybrids presented a stronger decrease of complex I compared with the controls, indicating that complex I is more unstable in the LHON mutants. Moreover, LHON cybrids characterized by different primary mutations displayed clear differences in complex I recovery kinetics. The 3460/*ND1* mutation exerted the mildest defect, whereas the 11778/*ND4* and 14484/*ND6* mutations hindered complex I assembly more severely. In addition to differences in complex I stability and assembly kinetics, clear differences were observed for the assembly and stability of complexes III and IV among LHON mutants characterized by different mtDNA backgrounds. In particular, the clone harboring the 11778/*ND4* mutation on a haplogroup U5a background showed, besides a strong complex I assembly defect, a severe impairment of complex IV and supercomplex $CIII_2$ + CIV assembly rates. This effect can only be explained by the presence of two mtDNA polymorphic variants affecting the *COIII* gene, G9477A and A9667G, (Table 1) which could add a deleterious effect to that of the 11778/*ND4* mutation. Unambiguously, the most affected clone was characterized by the 3460/*ND1* mutation on haplogroup H12 (ND1/H12), which showed a severe delay in the recovery rate of complexes III and IV, and consequently almost no expression of mitochondrial supercomplex $CIII_2$ + CIV. In contrast, the 3460/*ND1* clone with a haplogroup H* mtDNA (ND1/H*) showed normal assembly rates for complexes III and IV. These differences can be attributed to the presence in clone ND1/H12 of one specific non-synonymous variant (A14552G) affecting the complex I *ND6* gene (Table 1). This genetic variant, together with the 3460/*ND1* LHON mutation, might decrease the stability of mitochondrial respiratory chain complexes and/or supercomplexes, but additional experiments are required to fully confirm this hypothesis. Finally, no differences in the recovery rates of respiratory chain complexes III and IV were detected between controls and clones harboring LHON mutations on haplogroup J1, despite a mild delay in the formation of complex III that soon reached normal levels. This is a remarkable and unexpected result, especially when considering that one 14484/*ND6* clone carries an additional non-synonymous mutation in *ND6* (14279/*ND6*), which has been proposed as a primary LHON mutation in a family of Russian ancestry (30). In that case, the 14279/*ND6* mutation was found on a U4 mtDNA haplogroup. These results suggest, in contrast to what has been previously proposed (7,8), that the combined accumulation of *ND* and *CYTB* non-synonymous variants on specific haplogroup J clades may exert a protective effect on the stability of respiratory chain complexes and supercomplexes. This may support the association of haplogroup J with successful ageing (31), or reduced risk of Parkinson disease (32). However, this result does not explain the increased LHON penetrance of the 11778/*ND4* and 14484/*ND6* mutations on certain haplogroup J backgrounds and further studies are needed to properly elucidate this issue.

Based on the present results on defective complex I assembly kinetics, the phenotypic severity of LHON mutations would increase from 3460/*ND1*<14484/*ND6*<11778/*ND4*. Our data agree with those obtained by others (15), who observed a direct correlation between defects of complex I-driven ATP synthesis and the clinical severity of LHON mutations. However, considering the global recovery kinetics of all respiratory chain complexes, the severity of the

LHON mutations would increase from 14484/*ND6*<11778/*ND4*<3460/*ND1*. These results match the data obtained from the polarographic assessment of complex I activity defects, as well as the clinical criteria for ranking the pathogenic potential of each LHON mutation (10). In our cellular model, the 14484/*ND6* cybrids presented the best global respiratory chain assembly recovery. Accordingly, the highest frequency of spontaneous visual recovery is found in LHON patients carrying the 14484/*ND6* mutation, commonly associated with haplogroup J1. Thus, our results suggest that the differences found in the assembly kinetics of respiratory chain complexes III and IV amongst the mutant clones can be a contributing factor to the differences of disease expression.

This study may also provide a further scenario for understanding the pathogenesis of LHON. Under regular physiological conditions, it is likely that the synthesis of respiratory chain complexes reaches a balance between newly synthesized and degraded respiratory chain complexes to cope with the tissue energy demand. A possibility is that under certain stress conditions in which the respiratory demand increases, a rapid energy supply is achieved through an increased rate of synthesis and enzyme activation of respiratory chain complexes. On certain mtDNA genetic backgrounds, the primary LHON mutations may not only alter the assembly rate of respiratory chain complex I, but also affect the formation of complexes III and IV. It is very likely that this defective assembly adds a negative effect on complex I stability (27–29), worsening the complex I activity defect. This in turn would decrease complex I-driven ATP synthesis (15), and increase ROS production and apoptosis, as demonstrated in cybrids (16–19). Conversely, when normal conditions are recovered, restoration of respiratory chain complexes would lead to normal respiratory chain activities and ATP synthesis. Our data plead in favor of a spontaneous visual recovery in those LHON patients in whom the RGCs degeneration prompted by a lack of energy has not yet reached a critical threshold (10). In agreement, allotopic expression of nuclear-re-coded ND4 using a recombinant adenovirus-based vector led to a partial rescue of the mitochondrial OXPHOS deficiency caused by the G11778A mutation in the cybrid model (33).

Although mtDNA haplogroups have been previously suggested to contribute in disease predisposition, possibly by modulating ROS production as recently shown in mouse cells (34), our current study demonstrates that biochemical differences in OXPHOS assembly kinetics could be an additional contributing factor. Still key features of LHON such as the incomplete penetrance of LHON mutations, male prevalence, tissue specificity to RGCs, and the mitochondrial bioenergetics and dynamics in neurons cannot be fully explained by the mtDNA genetic background. Thus, the putative role of nuclear modifying genes or epigenetic/environmental factors in the pathogenesis of LHON requires further investigation. In this regard, the influence that different nuclear genetic backgrounds may exert on further modulating the assembly kinetics of the respiratory chain complexes in LHON cybrids with the same mtDNA background will aid future studies. The upcoming results on the assembly kinetics of respiratory chain complexes will provide essential information about the nature of mitochondrial respiratory chain deficiencies, and will enhance our understanding of OXPHOS disease mechanisms.

MATERIALS AND METHODS

Cell lines and culture conditions

Cybrid cell lines were constructed using the osteosarcoma 143B TK$^-$206 cell line as an acceptor rho zero cell line, and either enucleated fibroblasts from two healthy controls (CON/K and CON/H) and six LHON probands carrying the 3460/*ND1*, 11778/*ND4* and 14484/*ND6* LHON primary mutations, or platelets from two healthy controls (CON/T2 and CON/J1) as mitochondria donors (9). Cells were cultured in high-glucose DMEM (Life Technologies) supplemented with 10% fetal calf serum, 2 mM L-glutamine, 1 mM sodium pyruvate and antibiotics. To block mitochondrial translation, 15 μg/ml doxycycline were added to the culture medium. Cells were grown in exponential conditions and harvested at the indicated time points.

MtDNA sequencing and quantification of mtDNA copy number

The entire mtDNA sequences of LHON and control cybrid cell lines were determined and analyzed as previously reported (7,35,36). Relative quantification of mtDNA versus nDNA was performed by real-time PCR in a HT 7500 Real Time PCR System (Applied Biosystems, Foster City, CA, USA) as previously described with minor modifications (37). Briefly, total DNA was extracted from cultured cells with the QIAamp DNA Mini Kit (Qiagen GmbH, Hilden, Germany). For each sample, mtDNA and nDNA were quantified in the same reaction tube. MtDNA detection was performed by one set of primers (forward primer: 5′-CCA CGG GAA ACA GCA GTG ATT-3′, reverse primer: 5′-CTA TTG ACT TGG GTT AAT CGT GTG A-3′) and FAM-labeled TaqMan probe (5′-FAM-TGC CAG CCA CCG CG-MGB-3′) targeted to 12S ribosomal gene of mtDNA. For nDNA detection, a kit including a TaqMan VIC-labeled probe for the RNAse P nuclear gene was used (Human RNAse P PDAR; Applied Biosystems). Thermal cycler conditions were as follows: 50°C for 2 min, 95°C for 10 min, and 40 cycles of 95°C for 15 s and 60°C for 1 min. All samples were tested in duplicate at two levels of DNA concentration. The relative quantification of mtDNA versus nDNA was calculated by using a calibration curve consisting of serial dilutions of a stock solution made up of plasmids constructs with mtDNA 12S and RNAse fragments inserts. The mtDNA copy number was determined by division of the total DNA concentration by the weight of each plasmid molecule.

Mitochondria preparation

Mitochondrial membranes were isolated from cell cultures, as previously described with minor modifications (38). Briefly, cybrid clones were cultured until cells were ~70% confluent. Cells were harvested with trypsin, washed twice with phosphate-buffered saline (PBS), and re-suspended in 100 μl

PBS plus 100 μl of digitonin solution (4 mg/ml). The cell solution was kept on ice for 10 min to dissolve the membranes. One milliliter of cold PBS was added to the cells, which were spun for 10 min at 10 000 r.p.m. at 4°C. The supernatant was removed, the pellet washed one more time in 1 ml cold PBS, and the protein concentration was determined using the MicroBCA protein assay kit (Pierce). For the preparation of native mitochondrial complexes, pellets were solubilized in 100 μl buffer containing 1.5 M aminocaproic acid, 50 mM Bis–Tris, pH 7.0. Next, 2% (w/v) *n*-dodecyl β-D-maltoside was added and the cells were incubated on ice for 10 min. After centrifugation for 30 min at 13 000 r.p.m. at 4°C, the supernatant was combined with 10 μl of sample buffer (750 mM aminocaproic acid, 50 mM Bis–Tris, 0.5 mM EDTA, 5% Serva Blue G-250) prior to loading.

Blue native electrophoresis and IGA assays

Blue native 5–15% gradient gels were loaded with 40 μg of mitochondrial protein using 50 mM Bis–Tris as an anode buffer and 15 mM Bis–Tris/50 mM tricine containing 0.02% Serva Blue G-250 as a cathode buffer. After electrophoresis, proteins were transferred to a PROTAN® nitrocellulose membrane (Schleicher & Schuell) at 25 V, overnight, and probed with specific antibodies. Duplicate gels were further processed for second dimension 10% SDS–PAGE following previously described methods. (38).

For complex I IGA assay, gels were incubated for 2 h at room temperature with the following solutions: 2 mM Tris–HCl, pH 7.4, 0.1 mg/ml NADH, and 2.5 mg/ml NTB (nitrotetrazolium blue). Gels were washed in distilled water, scanned and photographed immediately.

Antibodies

Western blotting was performed using primary antibodies raised against the following subunits of the human mitochondrial OXPHOS complexes: NDUFA9 (39 kDa), UQCRC2, COX5A and SDHA, (Molecular Probes). Peroxidase-conjugated anti-mouse IgG was used as a secondary antibody (Molecular Probes). The signal was detected with ECL® plus (Amersham Biosciences) and the quantification of the blots was performed by using the ImagePro-Plus 4.1 image analysis software (Media Cybernetics, Silver Spring, MD, USA).

SUPPLEMENTARY MATERIAL

Supplementary Material is available at *HMG* Online.

FUNDING

This study was partially supported by Fundación de Investigación Biomédica del Hospital Universitario 12 de Octubre/Agencia Pedro Laín Entralgo, and Instituto de Salud Carlos III (ISCIII) to C.U. (grant numbers 04/00011 and PI05-0379), by Fundación ARAID and ISCIII to E.R.P. (PI05-0647), by a Telethon-Italy grant (#GGP06233) to V.C., by Progetti Ricerca Interesse Nazionale 2007 (Italian Ministry of the University) to A.T., and by Fundación de Investigación Médica Mutua Madrileña to M.A.M. (2005-069).

ACKNOWLEDGEMENTS

We thank Dr A. García-Redondo, A. Blázquez and A. Delmiro for useful discussions and technical support.

Conflict of Interest statement. None of the coauthors of the present manuscript have any financial interests or connections, direct or indirect, or other situations that might raise the question of bias in the work reported or the conclusions, implications, or opinions stated – including pertinent commercial or other sources of funding for the individual author(s) or for the associated department(s) or organization(s), personal relationships, or direct academic competition.

REFERENCES

1. Riordan-Eva, P., Sanders, M.D., Govan, G.G., Sweeney, M.G., Da Costa, J. and Harding, A.E. (1995) The clinical features of Leber's hereditary optic neuropathy defined by the presence of a pathogenic mitochondrial DNA mutation. *Brain*, **118**, 319–337.
2. Harding, A.E., Sweeney, M.G., Govan, G.G. and Riordan-Eva, P. (1995) Pedigree analysis in Leber hereditary optic neuropathy families with a pathogenic mtDNA mutation. *Am. J. Hum. Genet.*, **57**, 77–86.
3. Wallace, D.C., Singh, G., Lott, M.T., Hodge, J.A., Schurr, T.G., Lezza, A.M., Elsas, L.J. and Nikoskelainen, E.K. (1988) Mitochondrial DNA mutation associated with Leber's hereditary optic neuropathy. *Science*, **242**, 1427–1430.
4. Brown, M.D., Sun, F. and Wallace, D.C. (1997) Clustering of Caucasian Leber hereditary optic neuropathy patients containing the 11778 or 14484 mutations on an mtDNA lineage. *Am. J. Hum. Genet.*, **60**, 381–387.
5. Hofmann, S., Jaksch, M., Bezold, R., Mertens, S., Aholt, S., Paprotta, A. and Gerbitz, K.D. (1997) Population genetics and disease susceptibility: characterization of central European haplogroups by mtDNA gene mutations, correlation with D loop variants and association with disease. *Hum. Mol. Genet.*, **6**, 1835–1846.
6. Torroni, A., Petrozzi, M., D'Urbano, L., Sellitto, D., Zeviani, M., Carrara, F., Carducci, C., Leuzzi, V., Carelli, V., Barboni, P. *et al.* (1997) Haplotype and phylogenetic analyses suggest that one European-specific mtDNA background plays a role in the expression of Leber hereditary optic neuropathy by increasing the penetrance of the primary mutations 11778 and 14484. *Am. J. Hum. Genet.*, **60**, 1107–1121.
7. Carelli, V., Achilli, A., Valentino, M.L., Rengo, C., Semino, O., Pala, M., Olivieri, A., Mattiazzi, M., Pallotti, F., Carrara, F. *et al.* (2006) Haplogroup effects and recombination of mitochondrial DNA: novel clues from the analysis of Leber hereditary optic neuropathy pedigrees. *Am. J. Hum. Genet.*, **78**, 564–574.
8. Hudson, G., Carelli, V., Spruijt, L., Gerards, M., Mowbray, C., Achilli, A., Pyle, A., Elson, J., Howell, N., La Morgia, C. *et al.* (2007) Clinical expression of Leber hereditary optic neuropathy is affected by the mitochondrial DNA-haplogroup background. *Am. J. Hum. Genet.*, **81**, 228–233.
9. King, M.P. and Attardi, G. (1989) Human cells lacking mtDNA: repopulation with exogenous mitochondria by complementation. *Science*, **246**, 500–503.
10. Carelli, V., Ross-Cisneros, F.N. and Sadun, A.A. (2004) Mitochondrial dysfunction as a cause of optic neuropathies. *Prog. Retin. Eye Res.*, **23**, 53–89.
11. Vergani, L., Martinuzzi, A., Carelli, V., Cortelli, P., Montagna, P., Schievano, G., Carrozzo, R., Angelini, C. and Lugaresi, E. (1995) MtDNA mutations associated with Leber's hereditary optic neuropathy: studies on cytoplasmic hybrid (cybrid) cells. *Biochem. Biophys. Res. Commun.*, **210**, 880–888.
12. Hofhaus, G., Johns, D.R., Hurko, O., Attardi, G. and Chomyn, A. (1996) Respiration and growth defects in transmitochondrial cell lines carrying the 11778 mutation associated with Leber's hereditary optic neuropathy. *J. Biol. Chem.*, **271**, 13155–13161.

13. Cock, H.R., Tabrizi, S.J., Cooper, J.M. and Schapira, A.H. (1998) The influence of nuclear background on the biochemical expression of 3460 Leber's hereditary optic neuropathy. *Ann. Neurol.*, **44**, 187–193.
14. Brown, M.D., Trounce, I.A., Jun, A.S., Allen, J.C. and Wallace, D.C. (2000) Functional analysis of lymphoblast and cybrid mitochondria containing the 3460, 11778, or 14484 Leber's hereditary optic neuropathy mitochondrial DNA mutation. *J. Biol. Chem.*, **275**, 39831–39836.
15. Baracca, A., Solaini, G., Sgarbi, G., Lenaz, G., Baruzzi, A., Schapira, A.H., Martinuzzi, A. and Carelli, V. (2005) Severe impairment of complex I-driven adenosine triphosphate synthesis in Leber hereditary optic neuropathy cybrids. *Arch. Neurol.*, **62**, 730–736.
16. Wong, A., Cavelier, L., Collins-Schramm, H.E., Seldin, M.F., McGrogan, M., Savontaus, M.L. and Cortopassi, G.A. (2002) Differentiation-specific effects of LHON mutations introduced into neuronal NT2 cells. *Hum. Mol. Genet.*, **11**, 431–438.
17. Beretta, S., Mattavelli, L., Sala, G., Tremolizzo, L., Schapira, A.H., Martinuzzi, A., Carelli, V. and Ferrarese, C. (2004) Leber hereditary optic neuropathy mtDNA mutations disrupt glutamate transport in cybrid cell lines. *Brain*, **127**, 2183–2192.
18. Floreani, M., Napoli, E., Martinuzzi, A., Pantano, G., De Riva, V., Trevisan, R., Bisetto, E., Valente, L., Carelli, V. and Dabbeni-Sala, F. (2005) Antioxidant defences in cybrids harboring mtDNA mutations associated with Leber's hereditary optic neuropathy. *FEBS J.*, **272**, 1124–1135.
19. Ghelli, A., Zanna, C., Porcelli, A.M., Schapira, A.H., Martinuzzi, A., Carelli, V. and Rugolo, M. (2003) Leber's hereditary optic neuropathy (LHON) pathogenic mutations induce mitochondrial-dependent apoptotic death in transmitochondrial cells incubated with galactose medium. *J. Biol. Chem.*, **278**, 4145–4150.
20. Andrews, R.M., Kubacka, I., Chinnery, P.F., Lightowlers, R.N., Turnbull, D.M. and Howell, N. (1999) Reanalysis and revision of the Cambridge reference sequence for human mitochondrial DNA. *Nat. Genet.*, **23**, 147.
21. Ugalde, C., Vogel, R., Huijbens, R., van den Heuvel, B., Smeitink, J. and Nijtmans, L. (2004) Human mitochondrial complex I assembles through the combination of evolutionary conserved modules: a framework to interpret complex I deficiencies. *Hum. Mol. Genet.*, **13**, 2461–2472.
22. Ugalde, C., Janssen, R.J., van den Heuvel, L.P., Smeitink, J.A. and Nijtmans, L.G. (2004) Differences in assembly or stability of complex I and other mitochondrial OXPHOS complexes in inherited complex I deficiency. *Hum. Mol. Genet.*, **13**, 659–667.
23. Yadava, N., Houchens, T., Potluri, P. and Scheffler, I.E. (2004) Development and characterization of a conditional mitochondrial complex I assembly system. *J. Biol. Chem.*, **279**, 12406–12413.
24. Lazarou, M., McKenzie, M., Ohtake, A., Thorburn, D.R. and Ryan, M.T. (2007) Analysis of the assembly profiles for mitochondrial- and nuclear-DNA-encoded subunits into complex I. *Mol. Cell Biol.*, **27**, 4228–4237.
25. Carelli, V., Vergani, L., Bernazzi, B., Zampieron, C., Bucchi, L., Valentino, M., Rengo, C., Torroni, A. and Martinuzzi, A. (2002) Respiratory function in cybrid cell lines carrying European mtDNA haplogroups: implications for Leber's hereditary optic neuropathy. *Biochim. Biophys. Acta*, **1588**, 7–14.
26. Amo, T., Yadava, N., Oh, R., Nicholls, D.G. and Brand, M.D. (2008) Experimental assessment of bioenergetic differences caused by the common European mitochondrial DNA haplogroups H and T. *Gene*, **411**, 69–76.
27. Schagger, H., De Coo, R., Bauer, M.F., Hofmann, S., Godinot, C. and Brandt, U. (2004) Significance of respirasomes for the assembly/stability of human respiratory chain complex I. *J. Biol. Chem.*, **279**, 36349–36353.
28. Acin-Perez, R., Bayona-Bafaluy, M.P., Fernandez-Silva, P., Moreno-Loshuertos, R., Perez-Martos, A., Bruno, C., Moraes, C.T. and Enriquez, J.A. (2004) Respiratory complex III is required to maintain complex I in mammalian mitochondria. *Mol. Cell*, **13**, 805–815.
29. Diaz, F., Fukui, H., Garcia, S. and Moraes, C.T. (2006) Cytochrome c oxidase is required for the assembly/stability of respiratory complex I in mouse fibroblasts. *Mol. Cell Biol.*, **26**, 4872–4881.
30. Zhadanov, S.I., Atamanov, V.V., Zhadanov, N.I., Oleinikov, O.V., Osipova, L.P. and Schurr, T.G. (2005) A novel mtDNA *ND6* gene mutation associated with LHON in a Caucasian family. *Biochem. Biophys. Res. Commun.*, **332**, 1115–1121.
31. De Benedictis, G., Rose, G., Carrieri, G., De Lonlay, M., Falcone, E., Passarino, G., Bonafe, M., Monti, D., Baggio, G., Bertolini, S. *et al.* (1999) Mitochondrial DNA inherited variants are associated with successful aging and longevity in humans. *FASEB J.*, **13**, 1532–1536.
32. van der Walt, J.M., Nicodemus, K.K., Martin, E.R., Scott, W.K., Nance, M.A., Watts, R.L., Hubble, J.P., Haines, J.L., Koller, W.C., Lyons, K. *et al.* (2003) Mitochondrial polymorphisms significantly reduce the risk of Parkinson disease. *Am. J. Hum. Genet.*, **72**, 804–811.
33. Guy, J., Qi, X., Pallotti, F., Schon, E.A., Manfredi, G., Carelli, V., Martinuzzi, A., Hauswirth, W.W. and Lewin, A.S. (2002) Rescue of a mitochondrial deficiency causing Leber hereditary optic neuropathy. *Ann. Neurol.*, **52**, 534–542.
34. Moreno-Loshuertos, R., Acin-Perez, R., Fernandez-Silva, P., Movilla, N., Perez-Martos, A., Rodriguez de Cordoba, S., Gallardo, M.E. and Enriquez, J.A. (2006) Differences in reactive oxygen species production explain the phenotypes associated with common mouse mitochondrial DNA variants. *Nat. Genet.*, **38**, 1261–1268.
35. Achilli, A., Rengo, C., Magri, C., Battaglia, V., Olivieri, A., Scozzari, R., Cruciani, F., Zeviani, M., Briem, E., Carelli, V. *et al.* (2004) The molecular dissection of mtDNA haplogroup H confirms that the Franco-Cantabrian glacial refuge was a major source for the European gene pool. *Am. J. Hum. Genet.*, **75**, 910–918.
36. Ruiz-Pesini, E., Lapena, A.C., Diez-Sanchez, C., Perez-Martos, A., Montoya, J., Alvarez, E., Diaz, M., Urries, A., Montoro, L., Lopez-Perez, M.J. *et al.* (2000) Human mtDNA haplogroups associated with high or reduced spermatozoa motility. *Am. J. Hum. Genet.*, **67**, 682–696.
37. Crespo, M., Sauleda, S., Esteban, J.I., Juarez, A., Ribera, E., Andreu, A.L., Falco, V., Quer, J., Ocana, I., Ruiz, I. *et al.* (2007) Peginterferon alpha-2b plus ribavirin vs interferon alpha-2b plus ribavirin for chronic hepatitis C in HIV-coinfected patients. *J. Viral Hepat.*, **14**, 228–238.
38. Nijtmans, L.G., Henderson, N.S. and Holt, I.J. (2002) Blue native electrophoresis to study mitochondrial and other protein complexes. *Methods*, **26**, 327–334.